CARBON letters

Original Articles
Carbon Letters Vol. 28, 87-95 (2018)

Equilibrium and kinetic studies of an electro-assisted lithium recovery system using lithium manganese oxide adsorbent material

Dong-Hee Lee[1,*], Taegong Ryu[2,*], Junho Shin[3], and Young Ho Kim[1,♠]

[1]Department of Chemical Engineering and Applied Chemistry, Chungnam National University, Daejeon 34134, Korea
[2]Mineral Resources Research Division, Korea Institute of Geoscience and Mineral Resources, Daejeon 34132, Korea
[3]Department of Biological Engineering, Inha University, Incheon 22212, Korea

Article Info
Received 6 March 2018
Accepted 20 March 2018

♠Corresponding Author
E-mail: yh_kim@cnu.ac.kr
Tel: +82-42-821-5898
*The authors have contributed equally in discussions of the work, performing the experiments, and writing the paper.

Open Access
DOI: http://dx.doi.org/10.5714/CL.2018.28.087

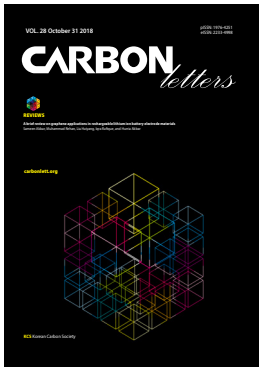

http://carbonlett.org

pISSN: 1976-4251
eISSN: 2233-4998

Abstract

This study examined the influence of operating parameters on the electrosorptive recovery system of lithium ions from aqueous solutions using a spinel-type lithium manganese oxide adsorbent electrode and investigated the electrosorption kinetics and isotherms. The results revealed that the electrosorption data of lithium ions from the lithium containing aqueous solution were well-fitted to the Langmuir isotherm at electrical potentials lower than –0.4 V and to the Freundlich isotherm at electrical potentials higher than –0.4 V. This result may due to the formation of a thicker electrical double layer on the surface of the electrode at higher electrical potentials. The results showed that the electrosorption reached equilibrium within 200 min under an electrical potential of –1.0 V, and the pseudo-second-order kinetic model was correlated with the experimental data. Moreover, the adsorption of lithium ions was dependent on pH and temperature, and the results indicate that higher pH values and lower temperatures are more suitable for the electrosorptive adsorption of lithium ions from aqueous solutions. Thermodynamic results showed that the calculated activation energy of 22.61 kJ mol^{-1} during the electrosorption of lithium ions onto the adsorbent electrode was primarily controlled by a physical adsorption process. The recovery of adsorbed lithium ions from the adsorbent electrode reached the desorption equilibrium within 200 min under reverse electrical potential of 3.5 V.

Key words: lithium recovery, lithium manganese oxide, electrosorption equilibrium, kinetic, isotherm

1. Introduction

The recovery of lithium from natural reservoirs is garnering significant attention because of the high demand for lithium, which is used in energy storage systems for portable electronic devices and electric vehicles [1-3]. Lithium can be recovered from various natural sources such as brines and ores [4], as well as the leaching solution of spent secondary lithium ion batteries [5,6]. Currently, various attempts have been made to recover lithium from solutions such as groundwater and seawater, which contain extremely low concentrations of lithium compared with other cations [7-11]. To recover lithium ions from seawater more effectively, it is important to develop an adsorbent that has a high lithium selectivity against other coexisting cations, such as potassium, calcium, and magnesium contained in seawater. In particular, lithium manganese oxide (LMO) with a spinel structure has been increasingly considered as an effective adsorbent because it can selectively recover lithium ions in an aqueous solution containing various cations [11-16]. Numerous efforts have been made towards the practical application of LMO adsorbent in aqueous solutions by the fabrication of composites using a polymeric

binder. The use of a polymeric binder, however, might cause a decrease in adsorption efficiency because of the obstruction of lithium ion transfer into the composite by the binder on the adsorbent surface. In addition, the acidic solution used in the desorption of adsorbed lithium ions may lead to structural damage by dissolution of manganese from the adsorbent and secondary environmental problems [15,16].

To overcome these challenges, we previously reported an electro-assisted lithium recovery system [17,18] using the concept of a modified membrane capacitive deionization (MCDI) process [19,20]. Compared with the conventional adsorption process using an adsorbent-binder composite, the recovery system with the electro-assisted method was noteworthy in that the lithium adsorption/desorption rates were improved, and the use of acidic solutions in the desorption process were not required. Moreover, a relatively excellent selectivity of lithium ions against other cations, such as potassium, sodium, calcium, and magnesium dissolved in seawater, was obtained [21].

In this study, we report in detail the isotherms and kinetics of the adsorption of lithium ions from aqueous solution under an electrical potential on the adsorbent electrode. We investigated the influence of the pH, temperature, applied potential, and lithium ion concentration experimental parameters. The classical Langmuir and Freundlich adsorption isotherms were used to understand the adsorption behavior of lithium ions during electrosorption, and the electrosorption rates were determined quantitatively using pseudo-first and second-order kinetics models. Moreover, we discuss the effect of electrosorptive potential on lithium ion recovery in terms of the recovered amount during the electro-desorption process. We expect that this experimental information will induce further development of electro-assisted lithium recovery systems for use in practical lithium ion recovery from such solutions as waste effluent, ground water, and seawater.

2. Experimental

2.1. Preparation of electrodes

The preparation procedure of the spinel-type $LiMn_2O_4$ powder (LMO) and adsorbent electrode used in this study was reported in our previous reports [18,21]. Briefly, the LMO was prepared through a solid-state reaction [22] using Li_2CO_3 (99%, Aldrich, USA) and $MnCO_3$ (99.9%, Aldrich) as the reactants. After mixing reactants at a lithium/manganese molar ratio of 1 of 2 by ball milling, the mixture was calcined at 500°C for 4 h in air. The calcined powder was then immersed into a 0.3 M HCl solution and stirred by a mechanical stirrer for 5 days to fully extract the lithium ions from the LMO framework through an H^+/Li^+ exchange reaction, which was confirmed by inductively coupled plasma (ICP) analysis [23]. The resulting LMO powder was washed with deionized water for several times until the filtrate reached a neutral pH, and then the filtered powder was collected and dried at 60°C overnight. Here, the resultant adsorbent powder is designated as HMO.

For the preparation of adsorbent electrodes, polyvinyl alcohol (PVA; molecular weight of 31,000–50,000, 98–99% hydrolyzed, Sigma-Aldrich) was used as a binder for the HMO powder. PVA dissolved in deionized water, glutaraldehyde (GA; 25wt%, Samchun Pure Chemical, Korea) as a cross-linking agent, and the HMO powder were mixed using a slurry mixer to obtain a homogeneous slurry. The slurry was then cast on a graphite sheet (Sigaflex, SGL Carbon, Germany) using a doctor blade (Mitutoyo, Japan) and dried at room temperature. To accelerate the esterification between the PVA and GA, an HCl solution was sprayed over the coated slurry. The electrode was then pressed using a roll press with a thickness of approximately 150 μm, and the loaded HMO on the graphite sheet (10 cm × 10 cm in size) was approximately 0.4 g.

As a counter electrode, an activated carbon powder (ACP; specific surface area of 1260 $m^2 g^{-1}$, Kuraray Chemical, Japan) electrode using poly(vinylidene fluoride) (PVdF; Sigma-Aldrich) as a polymeric binder was used for the experiment [24]. The total binder content in the ACP electrode was 15% dry weight. The thickness of the ACP composite layer was approximately 250 μm, and the loaded amounts of ACP on the graphite sheet (10 cm × 10 cm in size) was approximately 1.0 g.

2.2. Preparation of the test cell

The test cell was fabricated by modifying a conventional MCDI cell that consisted of two carbon electrodes, an anion exchange membrane and a dielectric spacer [19,24,25]. Fig. 1 shows a schematic diagram of the test cell and the system configuration of the experimental device. It consisted of the ACP electrode for anion capture, the HMO electrode for lithium ion adsorption, an anion exchange membrane (Neosepta AMX, Tokuyama Soda Corp.), a dielectric spacer (porous urethane foam, 200 μm thick), and the two acryl plates. The distance between the two electrodes in the assembly of the components was maintained at approximately 150 μm by a flexible dielectric spacer. The upper plate was designed to give two inlet holes at the corner and one outlet hole at the center of the plate with an inner diameter of 2 mm so that a solution could flow and contact the inner sides of the electrodes.

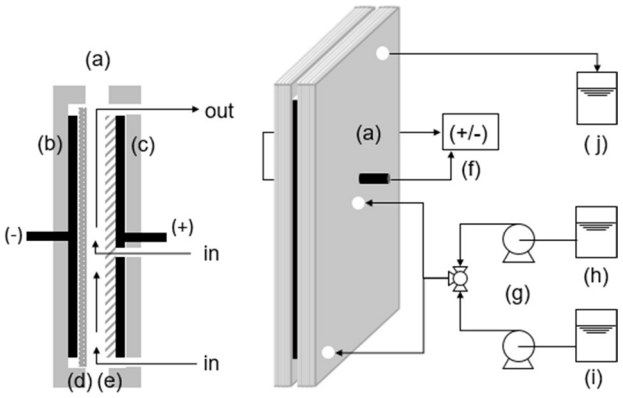

Fig. 1. Schematic view of the lithium recovery system using electrodes: (a) test cell, (b) activated carbon electrode, (c) HMO electrode, (d) anion exchange membrane, (e) porous urethane spacer, (f) potentiostat, (g) peristaltic pump, (h) Li-solution reservoir, (i) deionized water reservoir, and (j) effluent reservoir.

2.3. Electrosorption properties

We investigated the influences of pH, temperature, electrical potential, and concentration of lithium ions in the feed solution on the lithium ion adsorption performance of the HMO electrode. The solution was continuously fed using a peristaltic pump from an influent reservoir with a flow rate of 20 mL min^{-1}. The uptake of adsorbed lithium ions during the electrosorption process was calculated by the following equation [26]:

$$q_t\left(\frac{mg_{Li}}{g_{\_adsorbent}}\right) = \frac{(C_o - C_t)V}{m} \quad (1)$$

where q_t (mg g^{-1}) is the adsorbed amount at sampled time (t), C_o is the initial concentration of lithium ions, C_t is the concentration of lithium ions at sampled time (t), V is the solution volume (L), and m is the mass (mg) of the applied adsorbent. The concentration of lithium ions in the sampled solution was analyzed with an ICP-atomic emission spectrophotometer (ICP-AES; Optima 7300D, Perkin Elmer).

2.4. Adsorption kinetics

The adsorption kinetics were determined using the classical pseudo-first-order and pseudo-second-order adsorption kinetics equations [27-29], which are presented below.

$$\log(q_e - q_t) = \log q_e - \frac{k_1 t}{2.303} \quad (2)$$

$$\frac{t}{q_t} = \frac{1}{k_2 q_e^2} + \frac{t}{q_e} \quad (3)$$

where q_e and q_t are the amounts of adsorbed lithium ions (mg/$g_{\_adsorbent}$) on the HMO electrode at equilibrium and time t (min), and k_1 (min^{-1} or h^{-1}) and k_2 (g mg^{-1} min^{-1} or g mg^{-1} h^{-1}) are pseudo-first and second-order rate constants, respectively. The lithium concentration of the feed solution was varied from 10 to 500 mg L^{-1} under various applied potentials (0 to –1.2 V).

2.5. Adsorption isotherms

The adsorption behavior of lithium ions on the HMO electrode was described quantitatively using adsorption isotherms. The classical Langmuir and Freundlich isotherms were used to describe the model of adsorption/electrosorption. Both isotherms were plotted using the following equations by applying the experimental data.

$$\frac{c_e}{q_e} = \frac{1}{q_m K_L} + \frac{c_e}{q_m} \quad (4)$$

$$\ln q_e = \ln K_F + \frac{1}{n}\ln C_e \quad (5)$$

where q_e is the adsorbed amount of lithium ions at equilibrium (mg/$g_{\_adsorbent}$), q_m is the maximum adsorption capacitance corresponding to monolayer coverage (mg/$g_{\_adsorbent}$), K_L is the Langmuir constant related to sorption energy (enthalpy of adsorption), and C is the equilibrium concentration of lithium ions. K_F (L mg^{-1}) is the Freundlich constant, and 1/n is an indication of the adsorption tendency of the adsorbate.

2.6. Activation energy

The activation energy of the electrosorption of lithium ions onto the HMO electrode was calculated as a function of temperature using the Arrhenius model. The form of the model equation can be expressed as follows:

$$\ln k_2 = \ln A - \frac{E}{RT} \quad (6)$$

where k_2 is the pseudo-second-order rate constant, A is the Arrhenius constant, E is the activation energy of adsorption, R is the gas constant, and T is the temperature in Kelvin and E/R is the slope value of $\ln k_2$ versus 1/T.

3. Results and Discussion

3.1. Adsorption kinetics

The most important factor in the adsorption study is the mass transfer rate. Considering the electrosorptive ion adsorption on the surface of the electrode, the adsorption and insertion of lithium ions onto the HMO electrode can be divided into the following three steps: (1) the mass transfer of lithium ions from the solution to the interface of the electrode and electrolyte; (2) the transfer of ions to the solid surface; and (3) the diffusion of lithium ions into the lithium vacant sites on the adsorbent. Typically, as illustrated in Fig. 2a, the adsorption efficiency was highly affected by the concentration of lithium ions in the aqueous solution. In this system, the adsorbent-based lithium adsorption system might suffer from a slow adsorption rate when the concentration of lithium ions in the solution is low. On the other hand, the lithium adsorption rate can be improved under an applied electrical potential, as depicted in Fig. 2b, and the experimental results are shown in Fig. 3. As shown in Fig. 3, the adsorption rate and equilibrium capacity increased with applied electrical potential. These results indicate that the adsorption of lithium ions on the adsorbent was strongly affected by the electrical potential. The adsorption capacity increased with

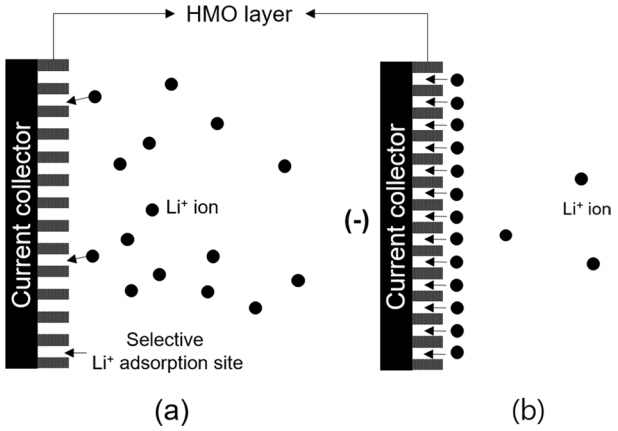

Fig. 2. Schematic illustration of lithium ion movements in solution (a) without electrical potential (physisorption) and (b) with electrical potential.

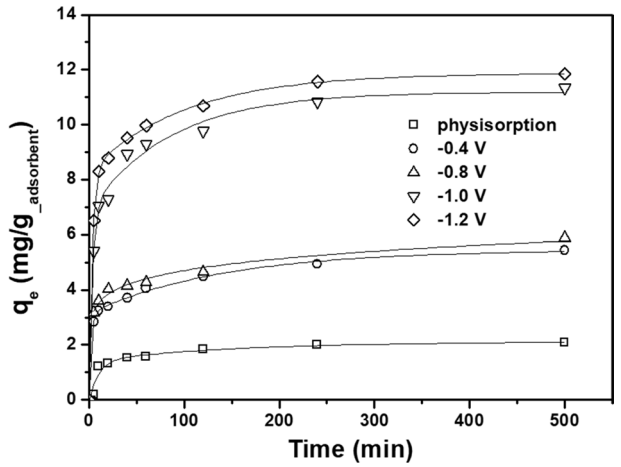

Fig. 3. Electrosorption capacities and rates of lithium ions with various applied electrical potentials.

an increasing electrical potential up to –1.2 V. Compared with physisorption without the electrical potential, the equilibrium capacity increased by 5.7 times at –1.2 V. Although the adsorption capacity did not increase proportionally with the electrical potential, we considered that the adsorption rate and capacity of lithium ions with respect to the HMO electrode depended on the electrical potential through the increasing electrostatic force [30].

The adsorption rate is important to understanding the lithium adsorption behavior on adsorbents. To examine the effect of applied electrical potential on lithium ion adsorption, the electrosorption was continued until the reaction reached a dynamic equilibrium (as determined by monitoring the conductivity of the effluent solution) to give the lithium ions full access to the HMO electrode. Fig. 4a shows the linearized plot fittings of the first-order kinetic model under the experimental conditions of 100 mg L^{-1} lithium ions in the feed solution at 25°C, and Fig. 4b shows the effect of different initial concentrations of lithium ions for electrosorption. The pseudo-first order kinetics model appeared to be well fitted for an adsorption potential of –0.4 V, as presented in Table 1; however, the coefficients of determination of the linearized plots under other conditions (R^2) did not match properly with that of the pseudo-first-order kinetics model. On the other hand,

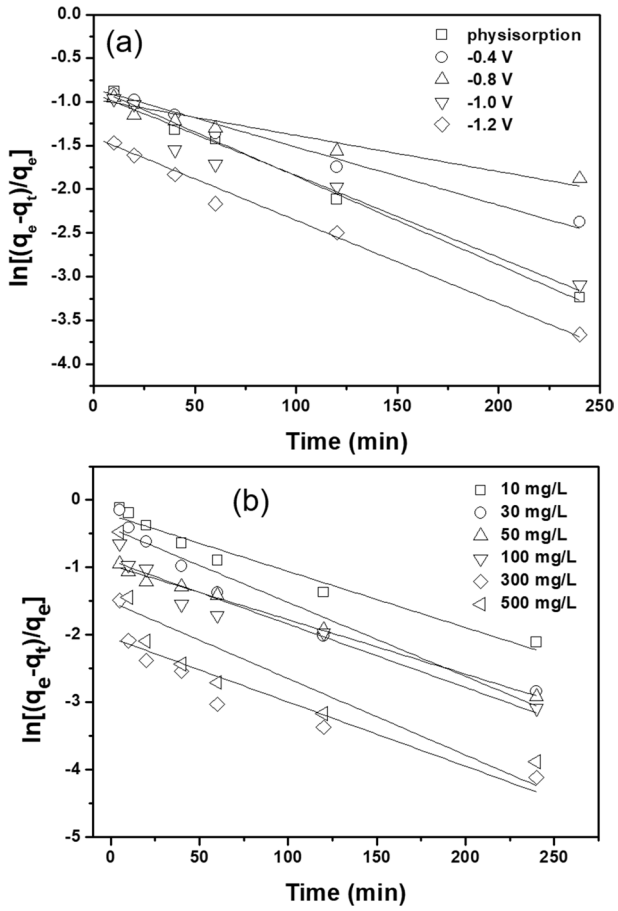

Fig. 4. Plots of the pseudo-first-order kinetics model with (a) different electrical potentials at 100 mg L^{-1} and (b) different initial concentrations of lithium ions at –1.0 V.

as shown in Fig. 5, the experimental data and the pseudo-second-order kinetic model were in good agreement for various electrical potentials and a wide range of initial lithium concentrations with the higher R^2 values of >0.99. Thus, the electrosorption kinetics of lithium ions on the adsorbent electrode more closely followed the pseudo-second-order model rather than the first-order model.

Table 1. Pseudo-first-order and pseudo-second-order parameters of the HMO and ACP electrodes system for the adsorption of lithium ions from aqueous solution under various applied voltages (T=25°C, C_o=100 mg L^{-1})

Applied potential	Pseudo-first-order model			Pseudo-second-order model		
	q_e (mg g^{-1})	k_1 (h^{-1})	R^2	q_e (mg g^{-1})	k_2 (g mg^{-1} h^{-1})	R^2
Physisorption	2.070	0.682	0.901	2.175	1.193	0.993
–0.4 V	5.436	0.400	0.969	5.510	0.682	0.996
–0.8 V	5.876	0.248	0.866	5.882	0.604	0.991
–1.0 V	11.335	0.564	0.929	11.506	0.444	0.999
–1.2 V	11.838	0.681	0.753	11.993	0.581	0.999

DOI: http://dx.doi.org/10.5714/CL.2018.28.087

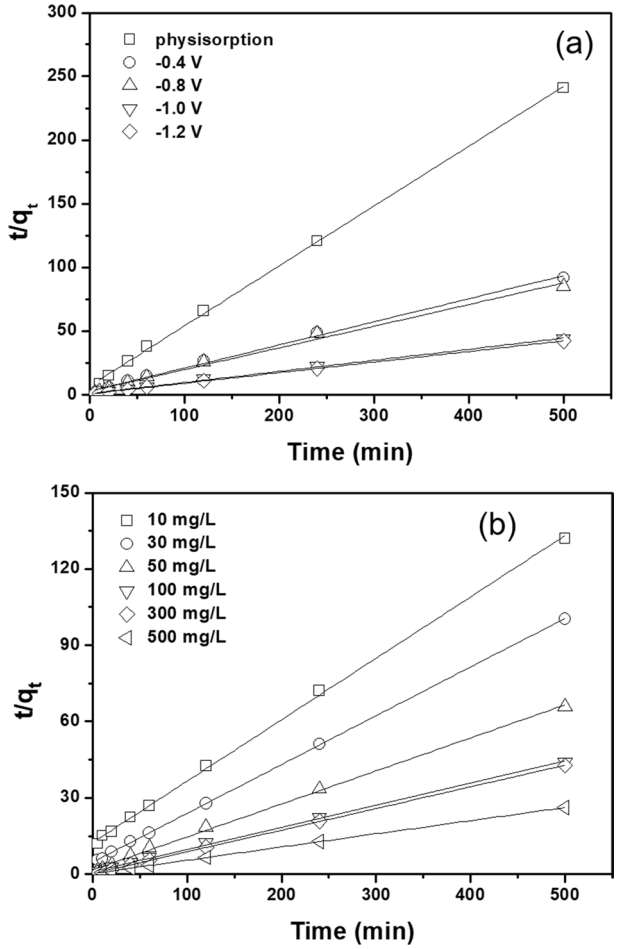

Fig. 5. Plots of the pseudo-second-order kinetics model with (a) different electrical potentials at 100 mg L^{-1} and (b) different initial concentrations of lithium ions at –1.0 V.

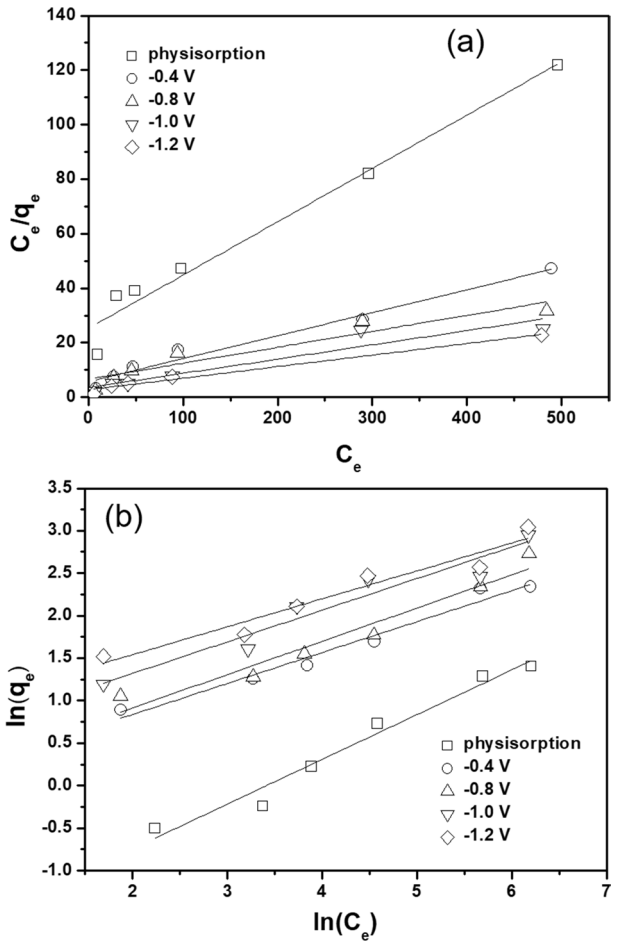

Fig. 6. Electrosorption isotherms of lithium ions with various applied voltages. (a) The Langmuir isotherm and (b) the Freundlich isotherm. (T of 25°C, V of 1000 mL, and adsorption time of 500 min).

3.2. Adsorption isotherms

Electrosorption is generally defined as the potential-induced adsorption onto the surface of electrodes [31]. Thus, it is important to understand equilibrium adsorption in designing an adsorption system under applied electrical potential. In this study, the adsorption behavior of lithium ions on the HMO electrode can be described quantitatively using the Langmuir and Freundlich adsorption isotherms. The Langmuir equation is the most commonly used isotherm because of its simplicity and capability to correlate a variety of adsorption experimental data into the isotherm model. To understand the effect of ion concentration and applied potential on the adsorption and/or electrosorption behavior, systematic experiments were conducted under various lithium concentrations of the feed solution (10 to 500 mg L^{-1}) and applied electrosorption potentials (physisorption to –1.2 V against the HMO and ACP electrode system). The linearized

Table 2. Parameters determined by plotting the Langmuir and Freundlich isotherms for the electrosorption performance of the HMO and ACP electrodes system

Applied potential	Langmuir			Freundlich		
	q_m	K_L	R^2	K_F	n	R^2
Physisorption	5.116	0.008	0.966	0.165	1.898	0.965
–0.4 V	11.898	0.015	0.972	1.116	2.746	0.965
–0.8 V	17.117	0.009	0.879	1.140	2.552	0.933
–1.0 V	19.139	0.015	0.879	1.777	2.684	0.914
–1.2 V	20.973	0.016	0.883	2.412	3.041	0.926

plots of Langmuir and Freundlich isotherms for lithium ions are presented in Fig. 6. The parameter values and correlation coefficients for the adsorption isotherms are presented in Table 2, which confirmed that all of the isotherm model parameters for the electrosorption of lithium ions in the HMO and ACP electrode system were well fitted for the two isotherm models. More specifically, according to the correlation coefficient (R^2), the Langmuir isotherm correlated better with the experimental data at the lower electrical potential range (< –0.4 V). On the other hand, the Freundlich isotherm correlated better at the higher electrical potential range (–0.8 to –1.2 V). These results indicate that monolayer adsorption was predominant at a low electrical potential, and multilayer adsorption was predominant at a high electrical potential because of the formation of a thicker electric double layer. Several studies have also applied the Freundlich equation to describe electrosorption in a capacitive system with high electrosorption potentials (> –1.0 V) [19,32]. However, it is difficult to explain the electrosorption mechanism using the classical Langmuir and Freundlich adsorption isotherm models because of the presence of an electrical potential. To explain the electrosorption phenomenon, various approaches have been employed. Biesheuvel et al. [33] suggested a modified Donann model that describes ion storage in the micropores of porous carbon materials such as activated carbon. Han et al. [34] suggested a quasi-equilibrium system that shows a Freundlich-like sorption behavior attributed to the micropore structure of the electrode material.

3.3. Effect of temperature

We investigated the effect of temperature on electrosorption in the range from 15 to 45°C at –1.0 V adsorption potential, and the results are represented in Fig. 7. It was found that the temperature of the feed solution had a significant effect on the adsorption performance. Moreover, a lower temperature was more favorable for lithium ion adsorption on the HMO electrode under an electrical potential, where the amount of adsorbed lithium increased from 6.65 mg/$g_{\_adsorbent}$ at 45°C to 12.66 mg/$g_{\_adsorbent}$ at 15°C. This might have been due to the interaction between the adsorbent and adsorbate becoming stronger at low temperatures [35,36]. Therefore, we concluded that a lower operation temperature might be advantageous for enhancing the adsorption capacity of lithium adsorption on the adsorbent electrode used in this system.

3.4. Activation energy

The pseudo-second-order rate constants were used to evaluate the spontaneity of the lithium adsorption on the HMO electrode during the electrosorption process and the type of interactions between the adsorbent and lithium ions. According to Eq. 6, k_2 was plotted versus 1/T, and a straight line with slope $-E_a/R$ was obtained. In the capacitive ion adsorption process, the magnitude of activation energy should provide information on the type of adsorption [37]. As shown in Fig. 8, the calculated Arrhenius activation energy was 22.61 kJ mol^{-1}. This indicates that the adsorption of lithium ions on the adsorbent electrode under application of an electrical potential was mainly dominated by physisorption rather than chemisorption (E > 40 kJ mol^{-1}) [38].

3.5. Effect of pH

Fig. 9 shows the electrosorption kinetics and electrosorption capacities of lithium ion solutions with various pH values. The pH of the solutions was adjusted using LiCl, LiOH, and HCl. The solution was purged with N_2 gas (99.999%) to remove the dissolved oxygen during the experiment. As shown in Fig. 9, the pH of the solution played a significant role in lithium ion electrosorption under an applied electrical potential of –1.0 V. The lithium ion uptake increased from 3.1 mg/$g_{\_adsorbent}$ at pH 5 to 11 mg/$g_{\_adsorbent}$ at pH 11. A lower solution pH reduced the lithium uptake, in which even the adsorbed lithium ions could be extracted from the adsorbent structure because of the competing ion exchange reaction between the protons in solution and the lithium ions on the adsorbent. The results showed that the adsorption rate and capacity decreased with a decreasing solution pH, which corresponded to the adsorption contribution to physisorption [39].

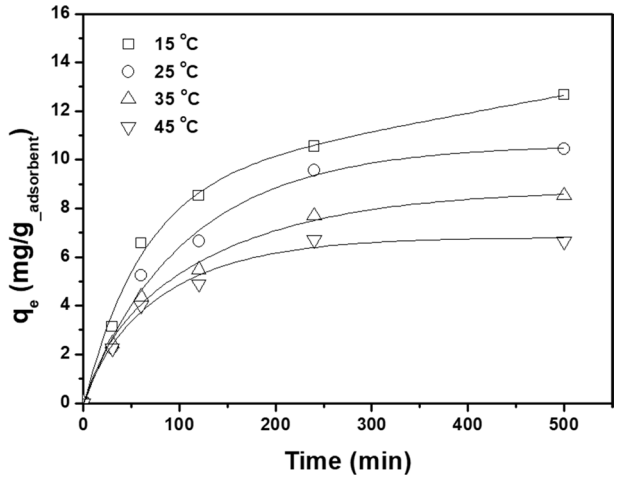

Fig. 7. Electrosorption kinetics of lithium ions at various solution temperatures.

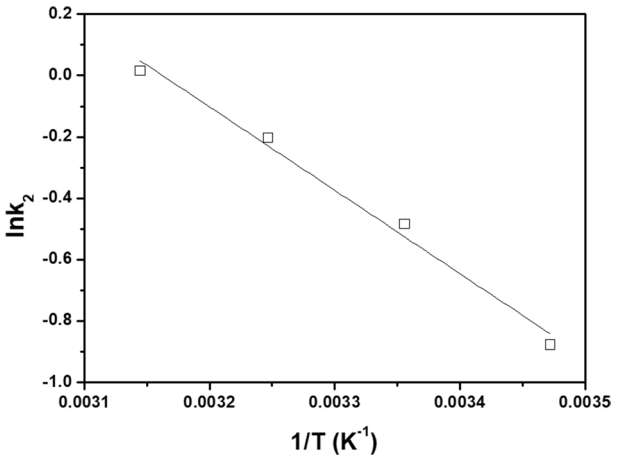

Fig. 8. Arrhenius plot for the activation energy of the electrosorption of lithium ions on the adsorbent-ACP electrodes system.

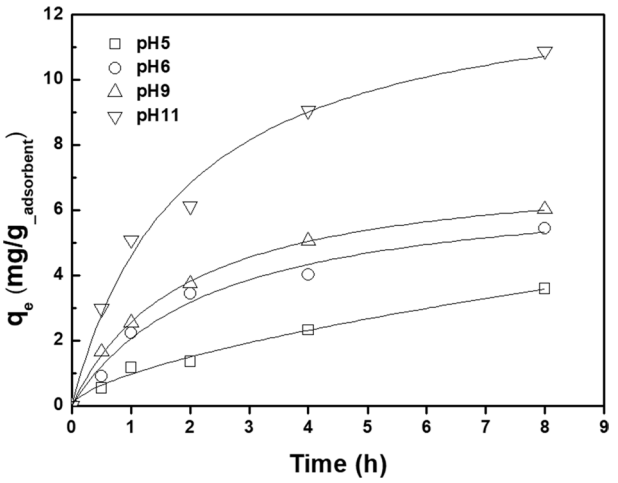

Fig. 9. Effect of pH on the electrosorption of lithium ions (T of 30°C; V of 200 mL; electrosorption for 8 h; a lithium concentration in the stock solution of 100 mg L^{-1}, and cell potential of –1.0 V).

3.6. Desorption characteristics

The electrodesorption kinetics was examined at a fixed electrical potential of 3.5 V. Before the tests, 100 mg L^{-1} of a LiCl solution was fed into the test cell, and the adsorption test was conducted by varying the electrical potential from physisorption to –1.2 V for 90 min. Then, the adsorbent electrode was washed with deionized water for 180 min to remove the lithium ions that were not adsorbed on the adsorbent electrode. The desorption equilibrium was reached within approximately 200 min for all cases and maintained at a nearly similar level up to 500 min, as shown in Fig. 10. This means that most of the lithium ions inserted into the adsorbent were desorbed at the earlier stage of electrodesorption (within 100 min) and slowly released afterwards. Moreover, the maximum amount of lithium (6.3 mg/$g_{adsorbent}$) desorbed when an adsorption potential of -1.2 V was applied, and this indicated that the adsorption capacity was dependent on the electrical potential for this electro-based lithium recovery process.

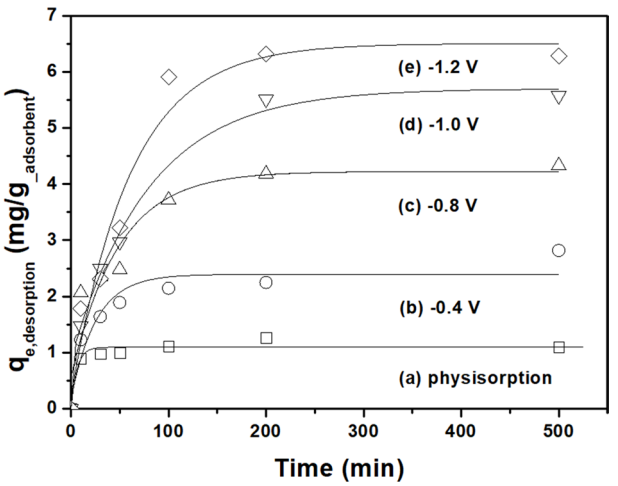

Fig. 10. Desorption rate of lithium ions from the adsorbent electrode under a reverse potential of 3.5 V. (a-e) indicate the applied adsorption potentials for the electrosorption process.

4. Conclusions

To understand the electrosorption behavior of lithium ions on an adsorbent electrode in the proposed electro-assisted lithium recovery system, we investigated the influence of experimental parameters, including pH, temperature, applied potential, and lithium ion concentration. The electrosorption capacity increased with an increasing electrostatic force. The experimental data were well matched with the Langmuir isotherm at potentials lower than –0.4 V and the Freundlich isotherm model at potentials higher than –0.4 V. The amount of adsorbed lithium ions decreased with an increasing solution temperature. The electrosorption kinetics well fit the pseudo-second-order kinetic model. The calculated activation energy was 22.61 kJ mol^{-1}, which indicated that the adsorption of lithium ions on the HMO surface was primarily consistent with physical adsorption. In the desorption process, adsorbed lithium ions were effectively recovered with an electrical potential of 3.5 V within 200 min from the effluent water.

Conflict of Interest

No potential conflict of interest relevant to this article was reported.

Acknowledgements

This work was also supported by the National Research Foundation of Korea (NRF) grant funded by the Korean government (MSIP) (NRF-2015R1A2A2A01002828).

References

[1] Diouf B, Pode R. Potential of lithium-ion batteries in renewable energy. Renewable Energy, 76, 375 (2015). https://doi.org/10.1016/j.renene.2014.11.058.

[2] Ren G, Ma G, Cong N. Review of electrical energy storage system for vehicular applications. Renewable Sustainable Energy Rev, 41, 225 (2015). https://doi.org/10.1016/j.rser.2014.08.003.

[3] Scrosati B, Hassoun J, Sun YK. Lithium-ion batteries: a look into the future. Energy Environ Sci, 4, 3287 (2011). https://doi.org/10.1039/C1EE01388B.

[4] Gruber PW, Medina PA, Keoleian GA, Kesler SE, Everson MP, Wallington TJ. Global lithium availability. J Ind Ecol, 15, 760 (2011). https://doi.org/10.1111/j.1530-9290.2011.00359.x.

[5] Meshram P, Pandey BD, Mankhand TR. Extraction of lithium from primary and secondary sources by pre-treatment, leaching and separation: a comprehensive review. Hydrometallurgy, 150, 192 (2014). https://doi.org/10.1016/j.hydromet.2014.10.012.

[6] Shuva MAH, Kurny ASW. Hydrometallurgical recovery of value metals from spent lithium ion batteries. Am J Mater Eng Technol,

1.8 (2013). https://doi.org/10.12691/materials-1-1-2

[7] Hong HJ, Park IS, Ryu T, Ryu J, Kim BG, Chung KS. Granulation of $Li_{1.33}Mn_{1.67}O_4$(LMO) through the use of cross-linked chitosan for the effective recovery of Li^+ from seawater. Chem Eng J, 234, 16 (2013). https://doi.org/10.1016/j.cej.2013.08.060.

[8] Park MJ, Nisola GM, Beltran AB, Torrejos REC, Seo JG, Lee SP, Kim H, Chung WJ. Recyclable composite nanofiber adsorbent for Li^+ recovery from seawater desalination retentate. Chem Eng J, 254, 73 (2014). https://doi.org/10.1016/j.cej.2014.05.095.

[9] Sagara F, Ning WB, Yoshida I, Ueno K. Preparation and adsorption properties of λ-MnO_2-cellulose hybrid-type ion-exchanger for lithium ion. Application to the enrichment of lithium ion from seawater. Sep Sci Technol, 24, 1227 (1989). https://doi.org/10.1080/01496398908049899.

[10] Umeno A, Miyai Y, Takagi N, Chitrakar R, Sakane K, Ooi K. Preparation and adsorptive properties of membrane-type adsorbents for lithium recovery from seawater. Ind Eng Chem Res, 41, 4281 (2002). https://doi.org/10.1021/ie010847j.

[11] Chung K, Lee J, Kim W, Kim S, Cho K. Inorganic adsorbent containing polymeric membrane reservoir for the recovery of lithium from seawater. J Membr Sci, 325, 503 (2008). https://doi.org/10.1016/j.memsci.2008.09.041.

[12] Feng Q, Miyai Y, Kanoh H, Ooi K. Lithium (1+) extraction/insertion with spinel-type lithium manganese oxides. Characterization of redox-type and ion-exchange-type sites. Langmuir, 8, 1861 (1992). https://doi.org/10.1021/la00043a029.

[13] Ooi K, Miyai Y, Katoh S, Maeda H, Abe M. Topotactic lithium (1+) insertion to. lambda.-manganese dioxide in the aqueous phase. Langmuir, 5, 150 (1989). https://doi.org/10.1021/la00085a028.

[14] Chitrakar R, Kanoh H, Makita Y, Miyai Y, Ooi K. Synthesis of spinel-type lithium antimony manganese oxides and their Li+ extraction/ion insertion reactions. J Mater Chem, 10, 2325 (2000). https://doi.org/10.1039/B002465L.

[15] Ma LW, Chen BZ, Chen Y, Shi XC. Preparation, characterization and adsorptive properties of foam-type lithium adsorbent. Microporous Mesoporous Mater, 142, 147 (2011). https://doi.org/10.1016/j.micromeso.2010.11.028.

[16] Shi X, Zhou D, Zhang Z, Yu L, Xu H, Chen B, Yang X. Synthesis and properties of $Li_{1.6}Mn_{1.6}O_4$ and its adsorption application. Hydrometallurgy, 110, 99 (2011). https://doi.org/10.1016/j.hydromet.2011.09.004.

[17] Ryu T, Ryu JC, Shin J, Lee DH, Kim YH, Chung KS. Recovery of lithium by an electrostatic field-assisted desorption process. Ind Eng Chem Res, 52, 13738 (2013). https://doi.org/10.1021/ie401977s.

[18] Ryu T, Lee DH, Ryu JC, Shin J, Chung KS, Kim YH. Lithium recovery system using electrostatic field assistance. Hydrometallurgy, 151, 78 (2015). https://doi.org/10.1016/j.hydromet.2014.11.005.

[19] Biesheuvel PM, van der Wal A. Membrane capacitive deionization. J Membr Sci, 346, 256 (2010). https://doi.org/10.1016/j.memsci.2009.09.043.

[20] Lee JH, Ahn HJ, Cho D, Youn JI, Kim YJ, Oh HJ. Effect of surface modification of carbon felts on capacitive deionization for desalination. Carbon Lett, 16, 93 (2015). https://doi.org/10.5714/CL.2015.16.2.093.

[21] Lee DH, Ryu T, Shin J, Ryu JC, Chung KS, Kim YH. Selective lithium recovery from aqueous solution using a modified membrane capacitive deionization system. Hydrometallurgy, 173, 283 (2017). https://doi.org/10.1016/j.hydromet.2017.09.005.

[22] Ryu T, Shin J, Ryu J, Park I, Hong H, Kim BG, Chung KS. Preparation and characterization of a cylinder-type adsorbent for the recovery of lithium from seawater. Mater Trans, 54, 1029 (2013). https://doi.org/10.2320/matertrans.M2013028.

[23] Han Y, Kim H, Park J. Millimeter-sized spherical ion-sieve foams with hierarchical pore structure for recovery of lithium from seawater. Chem Eng J, 210, 482 (2012). https://doi.org/10.1016/j.cej.2012.09.019.

[24] Kim YJ, Choi JH. Enhanced desalination efficiency in capacitive deionization with an ion-selective membrane. Sep Purif Technol, 71, 70 (2010). https://doi.org/10.1016/j.seppur.2009.10.026.

[25] Li H, Gao Y, Pan L, Zhang Y, Chen Y, Sun Z. Electrosorptive desalination by carbon nanotubes and nanofibres electrodes and ion-exchange membranes. Water Res, 42, 4923 (2008). https://doi.org/10.1016/j.watres.2008.09.026.

[26] Abbasi S, Noorizadeh H. Adsorption of Nile Blue A from aqueous solution by different nanostructured carbon adsorbents. Carbon Lett, 23, 30 (2017). https://doi.org/10.5714/CL.2017.23.030.

[27] Wan MW, Kan CC, Rogel BD, Dalida MLP. Adsorption of copper (II) and lead (II) ions from aqueous solution on chitosan-coated sand. Carbohydr Polym, 80, 891 (2010). https://doi.org/10.1016/j.carbpol.2009.12.048.

[28] Ho Y. Review of second-order models for adsorption systems. J Hazard Mater, 136, 681 (2006). https://doi.org/10.1016/j.jhazmat.2005.12.043.

[29] Ho YS, McKay G. Kinetic models for the sorption of dye from aqueous solution by wood. Process Saf Environ Prot, 76, 183 (1998). https://doi.org/10.1205/095758298529326.

[30] Chen Z, Song C, Sun X, Guo H, Zhu G. Kinetic and isotherm studies on the electrosorption of NaCl from aqueous solutions by activated carbon electrodes. Desalination, 267, 239 (2011). https://doi.org/10.1016/j.desal.2010.09.033.

[31] Huang SY, Fan CS, Hou CH. Electro-enhanced removal of copper ions from aqueous solutions by capacitive deionization. J Hazard Mater, 278, 8 (2014). https://doi.org/10.1016/j.jhazmat.2014.05.074.

[32] Biesheuvel PM. Thermodynamic cycle analysis for capacitive deionization. J Colloid Interface Sci, 332, 258 (2009). https://doi.org/10.1016/j.jcis.2008.12.018.

[33] Biesheuvel PM, Zhao R, Porada S, van der Wal A. Theory of membrane capacitive deionization including the effect of the electrode pore space. J Colloid Interface Sci, 360, 239 (2011). https://doi.org/10.1016/j.jcis.2011.04.049.

[34] Han L, Karthikeyan KG, Anderson MA, Wouters JJ, Gregory KB. Mechanistic insights into the use of oxide nanoparticles coated asymmetric electrodes for capacitive deionization. Electrochim Acta, 90, 573 (2013). https://doi.org/10.1016/j.electacta.2012.11.069.

[35] Li H, Pan L, Zhang Y, Zou L, Sun C, Zhan Y, Sun Z. Kinetics and thermodynamics study for electrosorption of NaCl onto carbon nanotubes and carbon nanofibers electrodes. Chem Phys Lett, 485, 161 (2010). https://doi.org/10.1016/j.cplett.2009.12.031.

[36] Wang HJ, Xi XK, Kleinhammes A, Wu Y. Temperature-induced hydrophobic-hydrophilic transition observed by water adsorption. Science, 322, 80 (2008). https://doi.org/10.1126/science.1162412.

[37] Mossad M, Zou L. A study of the capacitive deionisation performance under various operational conditions. J Hazard Mater, 213-214, 491 (2012). https://doi.org/10.1016/j.jhazmat.2012.02.036.

[38] Boparai HK, Joseph M, O'Carroll DM. Kinetics and thermodynamics of cadmium ion removal by adsorption onto nano zerovalent iron particles. J Hazard Mater, 186, 458 (2011). https://doi.org/10.1016/j.jhazmat.2010.11.029.

[39] Wang L, Meng CG, Han M, Ma W. Lithium uptake in fixed-pH solution by ion sieves. J Colloid Interface Sci, 325, 31 (2008). https://doi.org/10.1016/j.jcis.2008.05.005.